A Simulation Model for a Linear Drive of a Magnetic Levitating Transportation Vehicle

Dirk Brakensiek, Gerhard Henneberger

Abstract— **In this paper a simulation model for a linear drive of a magnetic levitating, autonomous transportation vehicle is presented. The vehicle is optionally supplied with a contactless energy- and information transmission. At the test bench of the vehicle measurements are made. The results of the model are verified by these measurements. According to this the model is used to develop a strategy of driving through horizontal curves only by controlling the motors.**

The commercial software *Matlab/Simulink* was used to build both, the model and the controller of the test bench. A *dSPACE* DSP controller board executes the real-time controller application.

The transportation system, the motor and the structure of the controller are explained. The results of the simulations driving on a straight line and comparisons to the measurements are given. Finally the simulation results of the curve-driving strategy are depicted.

Keywords— **Luggage-transportation system, magnetic levitating vehicle, linear drive, homopolar motor, simulation model, horizontal curve.**

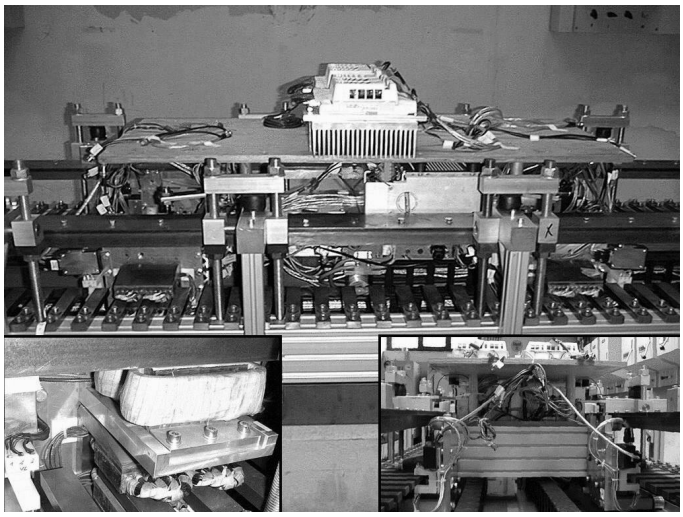

Fig. 1. The transportation system.

I. Introduction

MAGNETIC levitation combined with linear drives offers many advantages, such as high velocity, no wear and no maintenance. Therefore such a magnetic levitating vehicle provides a high reliability. Possible applications are conveyor systems for clean rooms or for the food industry or luggage transportation systems at airports. Because of the high velocity of the system the time e.g. between an arriving flight at an aiport and the connection flight can be halved. In the same way personnel costs for maintenance can be reduced significantly.

Since horizontal curves are necessary in luggage-transportation systems one has to develop a strategy to drive through them. In order to examine the behaviour of the vehicle a simulation model is build. The results of the simulation are compared to measurements made at the rectilineal test bench.

II. The Transportation System

The vehicle consists of a bogie and a luggage shell with a propulsion and levitation head on each corner of the bogie. A short-stator type linear homopolar motor has been chosen [1]. The levitation magnet is U-core shaped and hybrid excited. Permanent magnets compensate the static load of the vehicle, the current in the coils stabilizes the magnet in its working point. The levitation air gap is set according to the load of the vehicle in a way that the current is minimized [2]. In order to obtain higher reluctance forces for the lateral guidance the reaction rail is slotted. The power converters for levitation and propulsion are mounted on the vehicle. Eddy current sensors detect the levitation air gap. Three light barriers at each corner are used to detect the position of the vehicle at regular intervals of 10 mm. Every propulsion head is equipped with its own position encoder.

The track consists of two passive rails, one for levitation and lateral guidance and one for propulsion. The energy- and information transmission lines are situated below the motor. The motor itself is located below the levitation system. Fig. 1 displays the transportation system.

Due to the principle of motor, bearing magnets and energy- and data transmission the transportation system has no wear and therefore requires no maintenance. The passive tracks are cheap and easy to build.

D. Brakensiek and G. Henneberger are with the Department of Electrical Machines (IEM), Aachen Institute of Technology (RWTH), Schinkelstraße 4, 52056 Aachen, Germany, phone: +49 241 80-97636, fax: +49 241 80-92270. E-mail: Dirk.Brakensiek@iem.rwth-aachen.de, http://www.iem.rwth-aachen.de/~braken

III. The Homopolar Motor

The principle of the homopolar motor is shown in Fig. 2. Two rare-earth permanent magnets generate the excitation flux. The flux is guided by the flux concentrating pieces in the track and closes through the armature and the yoke. As a result the flux density under pole A is high whereas it is low under pole B. If the armature coils, designed as a conventional travelling-field winding, are fed with field-orientated current the propulsion force under pole A is high whereas it is low in the opposite direction under pole B due to the modulation of the flux density. The resulting force acts into the driving direction. The armature coils are fed with square-wave currents. The current commutates every

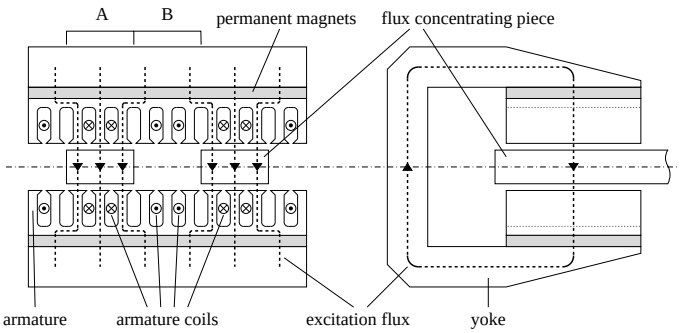

Fig. 2. Principle of the homopolar motor.

60° electrical to the next phase. Though the airgap is large the motor achieves a high efficiency.

IV. The Test Bench

The test bench consists of two parts, the vehicle with the track and the control interface. The controller application is executed on the DSP board and influenced by an operator via the PC. The position sensor signals are submitted to the DSP board using an electrical isolation. The controller algorithm switches the currents in the motor. The actual current is measured by a current transformer and is also submitted to the DSP. The structure of the test bench is displayed in Fig. 3.

V. The Controller Structure at the Test Bench

Fig. 6 shows the structure of the control system of the drive. It is a three stage cascade controller. The inner loop contains the current controller, the outer loops consist of the speed and position controller. The position and the speed controller are realised as PI controllers with output limitation and anti-windup loop. The current controller is implemented as a tolerance band controller. In addition a puls-width modulation current controller was considered. The performance of both current controllers is comparable, but using the puls-width modulation current controller the resulting noise produced by the motor is less than using the tolerance band current controller.

The position of each linear motor is detected by three light barriers in steps of 10 mm, which corresponds to an

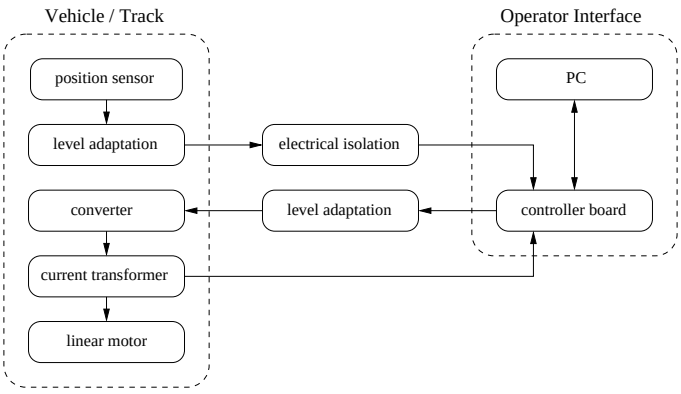

Fig. 3. Structure of the test bench.

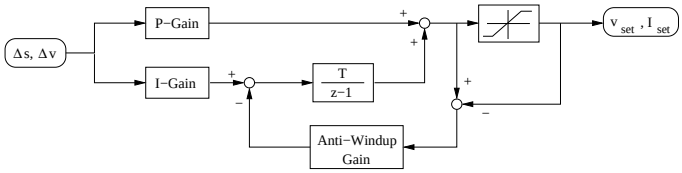

Fig. 4. The PI controllers with output limitation and anti-windup.

electrical angle of 60°. This position signal is filtered and the first derivative is used to obtain the actual speed v_{act}. The filter chosen is a 2nd order lowpass butterworth filter with a cut-off frequency of 10 Hz. The position signal is required also for the field-oriented control of the current.

The controllers, the generation of the setpoint value of the position, the filter and the differentiator are implemented within the software on the controller board. Inputs to the controller board are the position encoder signals and the actual current I_{act}, outputs are the gate control signals to the IGBT converter. As many parts as possible are realised within the software to achieve a great flexibility.

The structure of the position and the speed PI controller is displayed in Fig. 4. If the values between input and output of the output-limiter differ, the anti-windup gain reduces the integral part of the controller. This means, that anti-windup takes effect, when the output is limitated, e.g. at the beginning of a setpoint step-change. As a consequence of this an overshot of the controlled variable can be reduced. The behaviour of the system becomes more dynamic.

The reference input variable, i.e. the setpoint value of the position, is created by a driving program. The user can define any desired driving cycle with different stop positions and velocities. Every state in a cycle consists of a set position, a maximum velocity of the vehicle and a period of time for which the vehicle remains at the position. As well the vehicle can change its set velocity while driving. Fig. 5 shows the driving performance at the test bench. At a distance of 5 m for accelerating and retarding the maximum

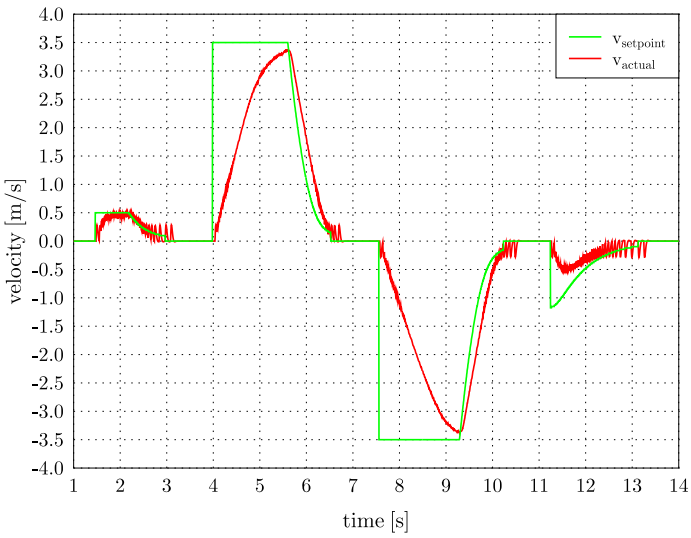

Fig. 5. Driving performance of the control system.

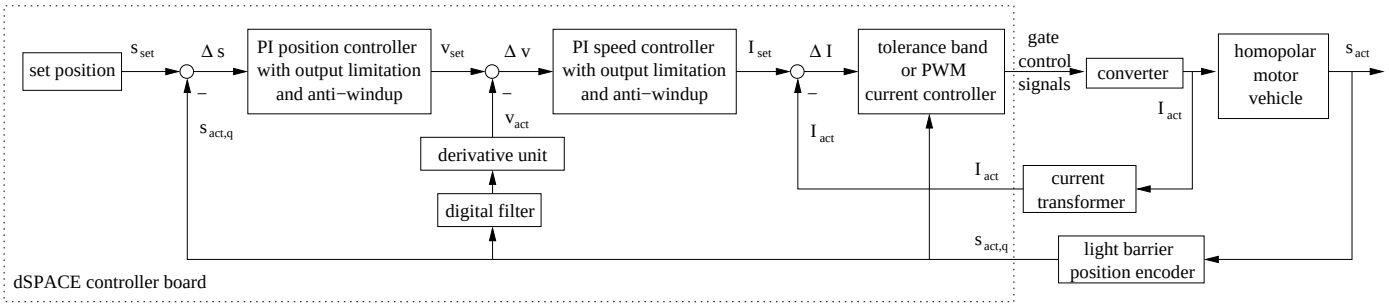

Fig. 6. Structure of the control system.

velocity is $3.3\,m/s$, the acceleration is $a = 3.13\,m/s^2$. The velocity pulses at slow speeds arise due to the coarse resolution of the position encoder. Due to this the controllers are turned off, if the position error is less than $\pm 35\,mm$.

VI. Model of the controlled system

The model and the controller as well were built using *Matlab/Simulink*. So identic parts such as the position and the speed controller, the derivative unit, the digital filter and the generation of the reference input variable were copied from the controller to the model. Current controller, converter and current transformer of the test bench are modelled as ideal devices. So it is assumed, that $I_{set} = I_{act}$. The controlled system consisting of homopolar motor, vehicle and position encoder has to be modelled. Thus the input of the controlled system is the actual current I_{act}, the output is the quantized actual position $s_{act,q}$.

The model of the controlled system is based on Newtons equation $a = \frac{F}{m}$, with m being the mass of the vehicle, F being the resulting propulsion force and a being the acceleration of the vehicle. The force of one motor depending on the current and the electrical angle results from FEM calculations, that are deposited in a two-dimensional look-up-table. The results of these FEM calculations are displayed in Fig. 7. A double integration of the acceleration leads to the actual position, s_{act}. The actual position is rounded

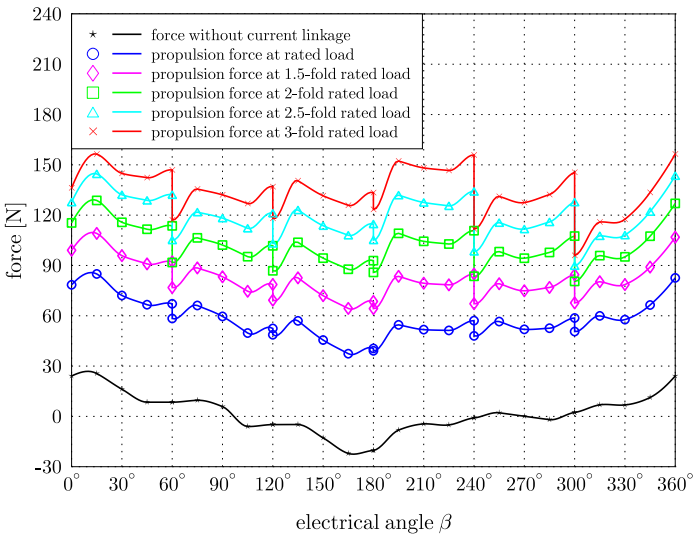

Fig. 7. Force of one motor, $F(I, \beta_{el})$.

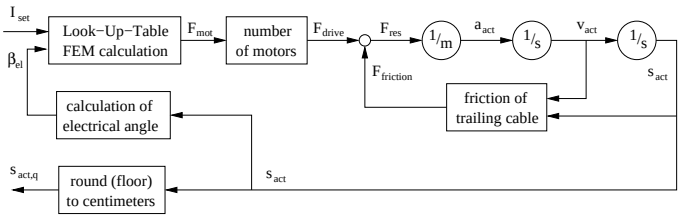

Fig. 8. Model of the controlled system.

to full centimeters, $s_{act,q}$, to model the quantization of the light barrier position encoder. In order to achieve the force of all motors, F_{drive}, the force of one motor, F_{mot}, is multiplied with the number of motors at the vehicle. In the current assembly of the test bench energy and information is transmitted to the vehicle by a trailing cable. So the force of all motors, F_{drive}, is reduced by the friction of this trailing cable. The friction force, $F_{friction}$, itself depends on the actual velocity and the actual position of the vehicle. The model of the controlled system is depicted in Fig. 8. It has to be mentioned that all motors are fed with the same current setpoint value and so far just driving on a straight line is possible. Only the distribution of the current to the phases differs from the front to the back motors, because there is a phase shift of 180° electrical between them. Each motor gets its phase angle from its own position encoder.

The parameters of the friction force of the trailing cable can not be measured. So they are adapted to obtain cor-

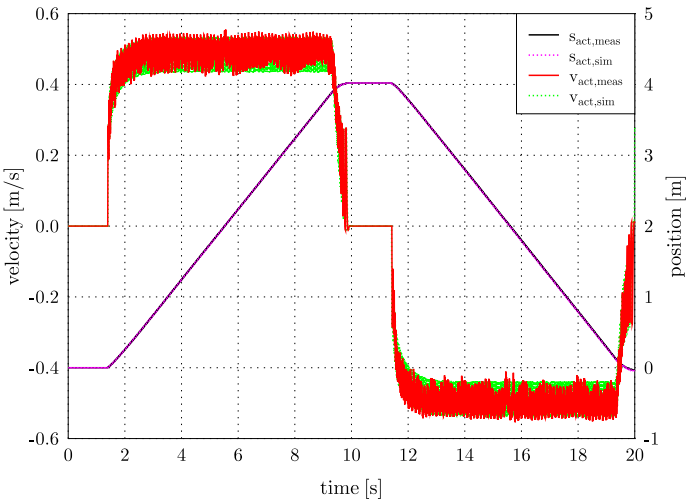

Fig. 9. Comparison of measurement and simulation.

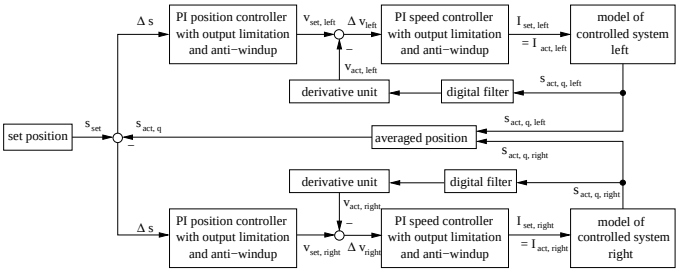

Fig. 10. Modified model for curve driving.

respondence between simulation and measurement. The comparison between simulated and measured actual velocity and actual position is shown in Fig. 9. There is no difference between them. In the same way simulation and measurement do not differ at other velocities, e.g. at $2\,m/s$.

VII. Simulation of the curve

In order to be able to pass horizontal curves a modified control strategy is necessary. The motors on the outside of the curve have to be faster than the inner motors. Therefore it is compulsory to fed the left and the right motors with different currents. At the test bench two converters are installed, one feding the left motors, the other feding the right motors. The model of the system is duplicated, one part controls the velocity of the left motors, the other part controls the velocity of the right motors. The modified model is shown in Fig. 10. The parts *model of controlled system left* and *model of controlled system right* are identical with Fig. 8. If the vehicle is located in the curve the setpoint values of the velocity between inner and outer motors, $v_{set,inner}$, $v_{set,outer}$, differ depending on inner and outer curve radius, r_{inner}, r_{outer}. With $v_{set,middle}$ being the vehicle's setpoint value of the velocity on the straight line and $b_{vehicle}$ being the width of the vehicle the velocities in the curve calculate as follows:

$$v_{set,inner} = v_{set,middle} \cdot \frac{r_{inner}}{(r_{inner} + b_{vehicle}/2)} \qquad (1)$$

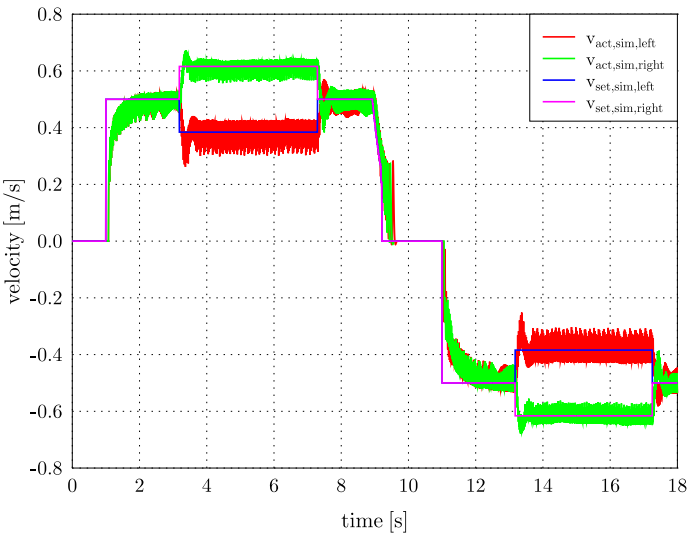

Fig. 11. Results of a curve driving simulation.

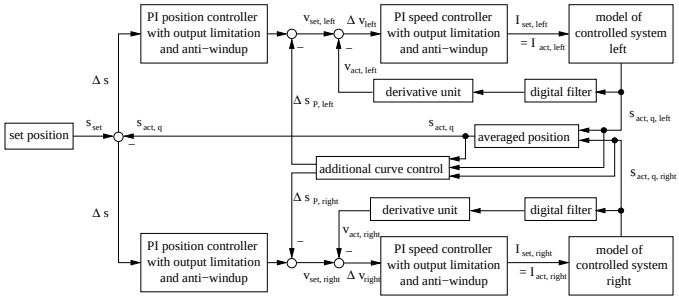

Fig. 12. Structure with additional controller.

$$v_{set,outer} = v_{set,middle} \cdot \frac{r_{outer}}{(r_{inner} + b_{vehicle}/2)} \qquad (2)$$

$$\frac{v_{set,inner}}{v_{set,outer}} = \frac{r_{inner}}{r_{outer}} \qquad (3)$$

The simulation results of driving through a horizontal curve with an inner curve radius of 1 m are depicted in Fig. 11. In this simulation at first the vehicle drives on a straight line with a velocity of 0.5 m/s, then enters a horizontal curve, leaves it again and stops on another straight line. After that it drives the same way back. At the stop position the calculated ideal positions of inner and outer motors differ from the simulated positions only by 20 mm, i.e. only two discretization steps.

One can define a quality factor that describes the deviation between a calculated ideal path of the vehicle and the simulated path of the vehicle. As soon as the vehicle enters the curve this quality factor has a peak because of the step change in the radius from infinity to 1 m, illustrated in the step change of the setpoint value of the velocity. As well by this simple method the steady state error of the quality factor is not zero. This means the vehicle has not rotated to the right position in the curve. So an additional controller was built that tries to minimize the peak error at the beginning of the curve and the steady state error. It is a simple P-controller that subtracts a certain value

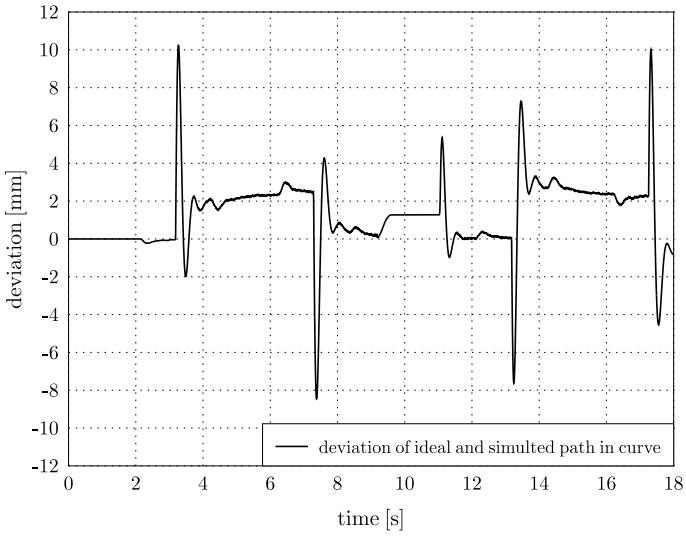

Fig. 13. Deviation between ideal and simulated path with additional controller and force loss in the curve.

proportional to the quality factor at the outputs of the position controllers. Fig. 12 shows the final block diagram of the system. The additional controller results in a halved peak of the quality factor at the beginning of the curve. A small steady state deviation can be achieved as well.

If the vehicle enters the curve the primary part of the motor and the flux concentrating pieces have a smaller overlapping than on the straight line. So the force of the motor has to be reduced in the model. This is done for each motor separately if it enters the curve. Fig. 11 and Fig. 13 show the complete simulation of the vehicle's velocity in the curve and the corresponding deviation between the calculated, ideal path and the simulated path of the vehicle. The deviation is less or equal to 10 mm, which is equivalent to a tipping angle of 0.5° between calculated, ideal path and simulated path. The disturbances are compensated very well. The pulses at the beginning and the end of the curve arise due to the sudden change of the radius, but their amplitude is small.

With the implementation of the curve at the test bench the simulations will be proved. Nevertheless a pre-test was sucessfully made: The right motors were driven forward and the left motors were driven backwards so that the vehicle should rotate. A turn of the vehicle could be noticed.

VIII. Conclusions

In this paper the design of a simulation model for a linear drive of a magnetic levitating, autonomous transportation vehicle was presented. The mechanical model was built as simple as possible but as precise as necessary. Measurements and simulations on a straight line correspond exactly. By the help of the model a strategy of driving through horizontal curves was developed. The vehicle manages the curve drive with minimal deviations from its ideal path.

References

[1] Wolfgang Evers, *Entwicklung von permanenterregten Synchronlinearmotoren mit passivem Sekundärteil für autonome Transportsysteme*, Ph.D. thesis, Fakultät für Elektrotechnik und Informationstechnik der RWTH Aachen, Verlag Shaker, 2000.

[2] Ingolf Gröning, *Magnetische Lagerung für ein autonomes Transportsystem mit normalkraftbehaftetem Linearantrieb*, Ph.D. thesis, Fakultät für Elektrotechnik und Informationstechnik der RWTH Aachen, Verlag Shaker, 2000.

[3] W. Evers, G. Henneberger, H. Wunderlich, A. Seelig, *A linear homopolar motor for a transportation system*, in *Proceedings of the 2nd International Symposium on Linear Drive for Industry Applications (LDIA 1998)*, Tokyo, Japan, 1998, pp. 46–49.

[4] D. Brakensiek, G. Henneberger, *Design of a Linear Homopolar Motor for a Magnetic Levitating Transportation Vehicle*, in *Proceedings of the 3rd International Symposium on Linear Drives for Industry Applications (LDIA 2001)*, Nagano, Japan, 2001, pp. 352–355.

[5] The MathWorks Inc., *Simulink*, Dynamic System Simulation for Matlab, *Using Simulink*, Version 4, Natrick, MA, USA, 2000

[6] dSPACE GmbH, *Control Desk* Experiment Guide, Paderborn, 2001

Dirk Brakensiek was born in Cologne, Germany, on December 27, 1973. After his schooling he studied electrical engineering from 1994 till 1999 at Aachen University of Technology. He graduated on the optimisation of a controller for a vertical transportation system. He got awards of ABB and Otto Junker GmbH. In November 1999 he began his Ph.D. studies at the Department of Electrical Machines. At first he worked on the electromagnetical optimisation of small-power motors. Now he is engaged on the drive of a magnetic levitating transportation vehicle.